Journal of Catalysis 392 (2020) 21–28

Contents lists available at ScienceDirect

Journal of Catalysis

journal homepage: www.elsevier.com/locate/jcat

Nanoceria as a recyclable catalyst/support for the cyanosilylation of ketones and alcohol oxidation in cascade

Francisco Garnes-Portolés [a,1], Miguel Ángel Rivero-Crespo [a,b,1], Antonio Leyva-Pérez [a,*]

[a] Instituto de Tecnología Química (UPV-CSIC), Universidad Politècnica de València-Consejo Superior de Investigaciones Científicas, Avda. de los Naranjos s/n, 46022 Valencia, Spain
[b] Department of Chemistry and Applied Biosciences, Swiss Federal Institute of Technology (ETH) Zürich, Vladimir-Prelog-Weg 1-5/10. 8093 Zürich. Switzerland[2]

ARTICLE INFO

Article history:
Received 3 September 2020
Revised 25 September 2020
Accepted 26 September 2020
Available online 8 October 2020

Keywords:
Nanoceria
Catalysis
Cyanosilylation
Aerobic oxidation of alcohols
Cyanohydrins

ABSTRACT

The cyanosilylation of carbonyl compounds is a fundamental reaction in organic synthesis, to give cyanohydrins. Ketones are particularly reluctant to cyanosilane addition and require the action of a catalyst, and despite many soluble Brönsted and Lewis acids have been employed for this task, it is difficult to find in the open literature catalytic solids able to carry out the reaction. Here, we show that commercially available nanoceria catalyzes the cyanosilylation of different ketones (21 examples) at temperatures between 0 and 50 °C, in high yields, under solventless conditions if required. The nanoceria network atoms act in a cooperative way to provide a bifunctional acid-base solid catalyst for the cyanosilylation reaction. The amorphization of nanoceria during reaction, due to acid release, does not hamper the catalytic activity and, indeed, different types of nanoceria, even with supported metal nanoparticles on surface, are active for the reaction, enabling extensive reuses after air calcination and the use of the catalytic material for the aerobic oxidation of alcohols / cyanosilylation reaction.

1. Introduction

The cyanosilylation of carbonyl compounds is the method of choice to synthesize cyanohydrins [1], versatile synthetic intermediates in organic synthesis with further reactivity through three adjacent functional groups: the cyano, silyl and carbonyl groups [2]. For instance, the cyanosilylation reaction is used in the pharmaceutical and agricultural industry to synthesize the pesticide Fenvalerate A and some non-steroid anti-inflammatory drugs, among others [3]. While aldehydes react with trimethylsilyl cyanide (TMSCN) without the need of a catalyst under certain conditions [4], ketones are more difficult to activate and always require the presence of a catalyst. For that reason, a wide variety of soluble Lewis acids have been employed to catalyze the cyanosilylation of ketones [1], habitually under heating conditions, and despite the plethora of catalytic systems reported for this reaction so far, it is difficult to find a solid catalyst able to efficiently perform the cyanosilylation of ketones at 25 °C or below [5].

The mechanism of the catalytic cyanosilylation reaction is widely described as an acid-base manifold, where the carbonyl and the cyanosilane compound are activated by the acid and its conjugated base, respectively [6]. This mechanism may, in principle, also occur on the surface of a bifunctional solid, such as a simple metal oxide [6b,c], provided that the latter shows the strong acidity required to activate the carbonyl group towards the cyanosilane [7]. Such an acid strength is not easy to achieve in a simple metal oxide, particularly for ketones, and besides, the stepwise cyanosilylation reaction releases corrosive HCN along the reaction, which may modify the structure of the metal oxide [8]. These drawbacks explain why only a reduced number of simple metal oxides catalyze the cyanosilylation reaction [9].

The advent of nanomaterials has brought new catalytic properties into old macroscopic solids [10,11]. Regarding metal oxides, when the size is reduced to the nanoscale, the metal site can be more accessible to external reagents by combining a higher solid surface area and a lower coordination number around the metal site, often accompanied by the generation of oxygen vacancies in the solid network [11a]. These new features in nanometal oxides invited us to explore their use as catalysts for the cyanosilylation reaction.

Here we show that a facile, high-yielding, room temperature cyanosilylation of ketones occurs with different types of crystalline nanosized cerium oxide as catalysts [12]. The nanoceria shows a high catalytic activity after calcination, to remove water and carbonates strongly adsorbed to the Ce^{4+} Lewis sites, with concomitant amorphization during use, which nevertheless does not

* Corresponding author.
E-mail address: anleyva@itq.upv.es (A. Leyva-Pérez).
[1] These authors contributed equally to the manuscript.
[2] Current address.

https://doi.org/10.1016/j.jcat.2020.09.032
0021-9517/

hamper the catalytic activity and tolerates extensive reuses. With this result in hand, the aerobic oxidation of alcohols/cyanosilylation reaction was performed with Au nanoparticles (NPs) supported on nanoceria.

2. Materials and methods

General. Reagents were obtained from commercial sources (Merck-Aldrich) and used without further purification otherwise indicated. Nanosized cerium oxide was purchased from Rhodia Co. The other nanoceria materials were prepared acording to previously published methods [13a]. The metal content of the solids was determined by inductively coupled plasma-atomic emission spectroscopy (ICP-AES) after disaggregation of the solid in *aqua regia* and later dilution, except for nanoceria where H_2O_2 (30 vol %) was used instead of the acid mixture. Dried and deaerated solvents were obtained after treatment with purification resins, having less than 50 ppm of water. All the products obtained were characterized by GC-MS, and ^1H, ^{13}C NMR, and DEPT were used in some cases to further confirm the product structure. When available, the characterization given in the literature was used for comparison. Gas chromatographic analyses were performed in an instrument equipped with a 25 m capillary column of 1% phenylmethylsilicone. GC-MS analyses were performed on a spectrometer equipped with the same column as the GC and operated under the same conditions. NMR were recorded in a 300 MHz instrument using the appropriate solvent containing TMS as an internal standard. Absorption spectra in solution were recorded on open cells in an UV/Vis spectrophotometer. Solid IR spectra were recorded on a spectrophotometer by previous mixture of the solid with dried KBr. Thermogravimetric analyses were performed on 0.5–0.8 mm pelletized samples under a dry N_2 atmosphere with a thermobalance operating at a heating rate of 10 °C·min^{-1}. N_2 adsorption-desorption isotherms were performed at 77 K on sieved materials after outgassing for 16 h under vacuum. Electron microscopy studies were performed on a microscope operated at 100–200 kV after impregnating a dispersion of the solid sample on a Cu grid and leaving to evaporate for, at least, 4 h.

Typical reaction procedure for cyanosilylation reactions with nanoceria. In a typical cyanosilylation reaction, 10 to 20 wt% of nanoceria catalyst was weighed under nitrogen in a 2 ml glass vial equipped with a magnetic stirrer. Then, 0.3 ml of *n*-hexanes, 0.25 mmol of carbonyl compound and 0.3 mmol of TMSCN were added, the vial was capped, and the mixture magnetically stirred at 25 °C for the indicated time. The final composition of the mixture was analyzed by GC-MS, and the conversion and selectivity were determined by GC using *n*-nonane or *n*-dodecane as an external standard.

Typical reaction procedure for the aerobic oxidation of alcohols/-cyanosilylation reaction catalyzed by Au-nCeO_2. The corresponding alcohol (4.85 mmol) was added over Au-nCeO_2 catalyst (200 mg, 1 Au mol%, 30 wt% nCeO_2; in cases where the alcohol is solid, 6 ml of hexane were also added, 0.8 M) in a glass reactor equipped with a stirring bar at 5 bar of O_2, and the resulting mixture was then heated at 80 °C for 5 h. After the reaction, acetone was added and the catalyst was separated by centrifugation. The mixture was analyzed by GC-MS, and the conversion and selectivity were determined by GC using *n*-nonane or *n*-dodecane as an external standard. The used catalyst was calcinated at 400 °C for 4 h, and introduced in a flask (20 mg, 2.4 Au%) with the synthesized ketone (0.42 mmol) and TMSCN (0.5 mmol), and the mixture was stirred at 25 °C for 8 h. The products in solution were analyzed by GC-MS, and conversion and selectivity were determined by GC using *n*-nonane or *n*-dodecane as an external standard.

3. Results and discussion

3.1. Cyanosilylation catalyzed by nanoceria

Table 1 shows the results for the cyanosilylation of acetophenone **1** with TMSCN **2** after 1 h reaction time, with different catalytic nanomaterials and solvents. It can be seen there that the reaction does not proceed without a catalyst nor in the presence of some representative nanoparticulated metal oxides, such as silicoalumina, titania nor zirconia (entries 1–4), but the reaction proceeds well with commercially available nanoceria catalyst (entry 5), at 25 °C and with *n*-hexanes as a solvent.

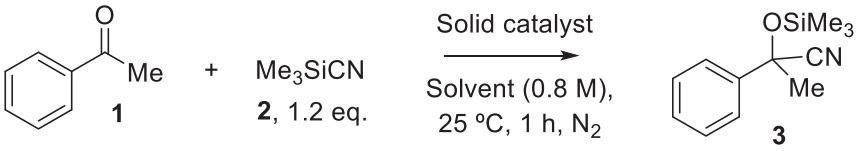

The solid acids were calcined at 400 °C prior to reaction, since otherwise no catalysis occurs, and Fig. 1A shows a high resolution-transmission electron microimage (HR-TEM) of the catalytic nanoceria after this treatment (higher resolution microimages of this commercially available material can be found elsewhere) [12d]. The material consists in crystalline NPs of ~7 nm particle size, without any water adsorbed on surface. Different organic solvents can be used (entries 5–10), although with less efficiency than *n*-hexanes, and the same yield of **3** is obtained when decreasing the amount of nanoceria from 50 to 20 wt% (entries 11–13). A tentative explanation on the solvent effect might be that the relative concentration of starting materials increases in the proximity of the catalyst surface when the most apolar solvent of all the solvents tested, i.e. *n*-hexanes, is used, which makes the reaction go faster. This explanation is supported by the fact that the reaction works faster under neat conditions (see ahead). Kinetic studies (Fig. S1) show that the yield of **3** nearly achieves a plateau after 20 min reaction time regardless the amount of solid catalyst employed (20 and 50 wt%), and filtration at 20% conversion stops the reaction completely, which strongly supports that the cyanosilylation of **1** is heterogeneously catalyzed by nanoceria (Fig. S2).

The yield of **3** is further increased by calcination of nanoceria at > 400 °C (entry 14), regardless if the calcination atmosphere is air, vacuum or N_2, and yields only decrease at calcination temperatures > 600 °C (Fig. S3). In contrast, calcination at 600 °C did not increase the yield of **3** for nanotitania and nanozirconia (entries 3–4 in Table 1). Thermogravimetric analyses show that the weight loss in nanoceria does not only correspond to the typical adsorbed water but also to strongly adsorbed species at 500 °C (Fig. S4), and

Table 1
Results for the cyanosilylation reaction of acetophenone **1** with TMSCN **2** catalyzed by nanoparticulated solid acids, calcined at 400 °C, after 1 h at 25 °C under inert atmosphere.

Entry	Solid catalyst (wt%)	Solvent	3 (yield, %)
1	None	*n*-Hexanes	0
2[a]	nanoSiO_2·Al_2O_3 (20 wt%)	*n*-Hexanes	5
3[b]	nanoTiO_2 (20 wt%)	*n*-Hexanes	18 (9)
4[b]	nanoZrO_2 (20 wt%)	*n*-Hexanes	1 (1)
5[c]	nanoCeO_2 (50 wt%)	*n*-Hexanes	58
6		Toluene	39
7[d]		DCM	27
8		Diethyl ether	42
9[d]		DMF	18
10[d]		THF	7
11	nanoCeO_2 (30 wt%)	*n*-Hexanes	56
12	**nanoCeO_2 (20 wt%)**	***n*-Hexanes**	**55**
13	nanoCeO_2 (10 wt%)	*n*-Hexanes	26
14[b,e]	**nanoCeO_2 (20 wt%)**	***n*-Hexanes**	**(67)**
15[b]	**nanoCeO_2 (20 wt%)**	**–**	**(72)**

[a] 13 wt% alumina.
[b] Between parentheses, result for the solid catalyst calcined at 600 °C.
[c] <5% of **3** with non-calcined solid.
[d] DCM stands for dichloromethane, DMF for *N,N*-dimethylformamide and THF for tetrahydrofurane.
[e] 61% and 58% of **3** at 0 °C and 50 °C reaction temperature, respectively.

Fourier-transformed infrared spectroscopy (FT-IR, Fig. S5) shows the progressive disappearance with the calcination temperature of the band corresponding to adsorbed carbonates (1384 cm^{-1}) and a shift of the band corresponding to atmospheric CO_2 (1690 cm^{-1}) [14]. The combined kinetic and IR results suggest that the removal of adsorbed carbonates is essential for nanoceria to act as a catalyst in the cyanosilylation of acetophenone **1**. Indeed, an induction time for the reaction was observed when lower calcination temperatures were employed, which may correspond to the time required for the desorption of carbonates. Together, these results strongly support that the Lewis acidity required for the cyanosilylation reaction is only achieved on the nanoceria surface after removal of the strongly adsorbed water and carbonate molecules, which may constitute a simple strategy to use nanoceria as a strong acid catalyst in organic synthesis.

Fig. 2A shows that the nanoceria catalyst is still very active for the cyanosilylation of **1** at 0 °C (see also Table 1, entry 14), and Fig. 2B shows that the reaction can also be run without any solvent, which is a clear advantage from an industrial point of view, to achieve a 72% yield after 1 h (see also Table 1, entry 15). Fig. 2C shows that the used solid catalyst is not active after simple washings with *n*-hexanes, and the corresponding FT-IR spectrum (Fig. S5) shows the appearance of new bands between 1100 and 1450 cm^{-1}, assignable to remaining organic impurities, which may block the active sites and produce the rapid deactivation of the catalyst at ~60% conversion. Since a simple calcination should remove these organic impurities, the used nanoceria catalyst was calcined at 400 °C to recover full activity for, at least, 10 uses, as shown in Fig. 2D, without any significant depletion of the intrinsic catalytic activity, as indicated by the similar initial rates. Notice that a higher calcination temperature is not required to recycle

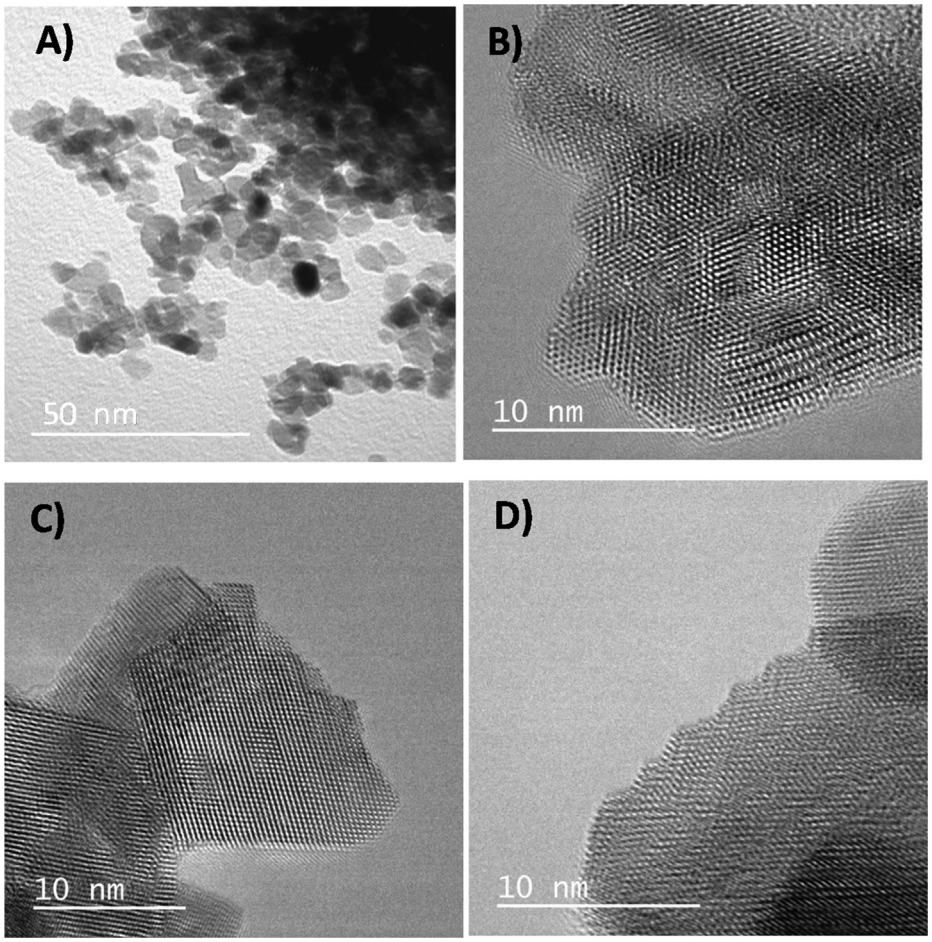

Fig. 1. High resolution-transmission electron microimages (HR-TEM) of commercially available nanoceria (A) and in-house synthesized ceria nanorods (B), nanooctahedra (C) and nanocubes (D), after calcination at 400 °C under air.

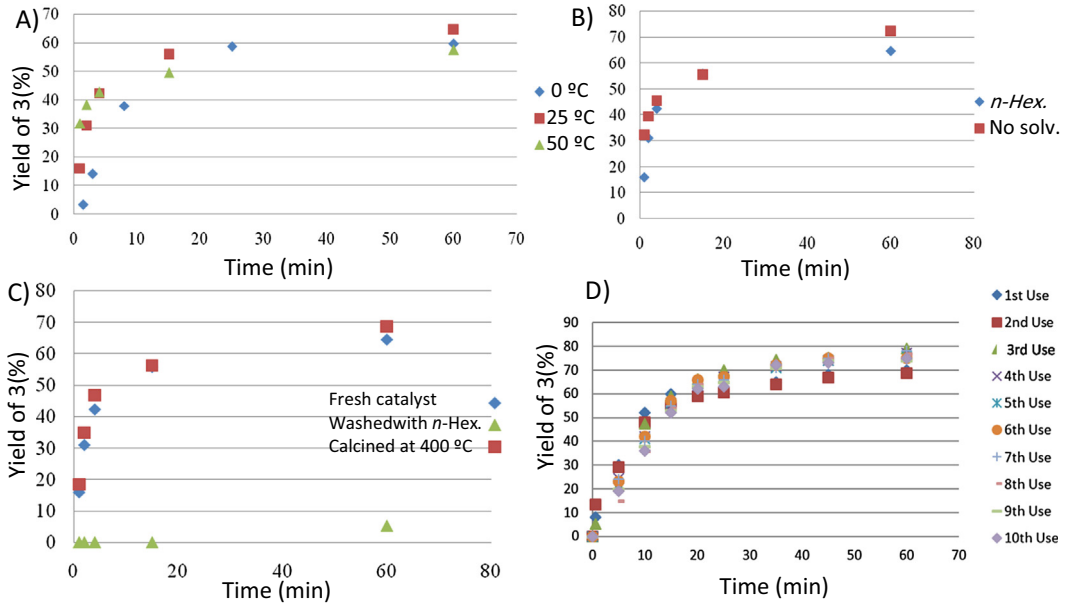

Fig. 2. (A) Kinetics for the cyanosilylation reaction of acetophenone **1** with TMSCN **2** at different reaction temperatures, under inert atmosphere and catalyzed by nanoceria (20 wt%) calcined at 600 °C. (B) With and without solvent. (C) Reuse of nanoceria after washing or calcination. (D) Yield-time plot for 10 uses of the nanoceria catalyst, after calcination.

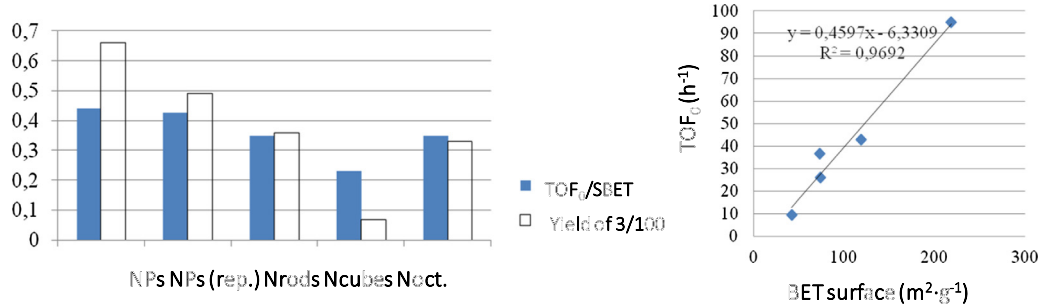

Fig. 3. Initial turnover frequency (TOF_0) *vs.* the Brunauer, Emmett and Teller (BET) surface of the different nanoceria catalysts for the cyanosilylation reaction of acetophenone **1** with TMSCN **2** at 25 °C and under inert atmosphere. Yields refer to 1 h reaction time.

the solid since carbonates are not present any more in the used catalyst according to the FT-IR spectrum, and only organic impurities must be removed.

The catalytic activity of a nanocrystalline solid often depends on the crystallographic face exposed to reactants.[13a] To check if that is the case here, ceria nanorods, nanooctahedra and nanocubes, which expose on surface the 111, 110, and 100 crystallographic planes, respectively, were prepared, and representative microimages are shown in Fig. 1B–D (see Fig. S6 for further images and Table S1 for calcination procedures and corresponding BET surface areas) [13,15]. The catalytic results for these materials, shown in Fig. 3, indicate that the catalytic activity linearly correlates with the total surface area of nanoceria and does not have any apparent relationship with the exposed face.

Nanoceria is well-known to possess a high number of oxygen vacancies [16]. However, the fact that the crystalline phase is irrelevant for the catalysis here, suggests that oxygen vacancies will most probably not play any role during the catalytic cyanosilylation, since a change in the crystalline phase of nanoceria implies a significant change in the oxygen vacant number (Table S2) [16a]. To further check this, the number of oxygen vacancies in nanoceria was increased by doping with different atoms, including metals (Ga, Sm, Al and Fe) [17] and by treatment with HCl [18]. These materials were used as catalysts under typical reaction conditions and the results show a decrease of the catalytic activity for all the doped nanoceria materials tested, thus strongly suggesting the lack of any catalytic role for oxygen vacancies (Fig. S7). To further confirm this point, 3,3́,5,5́-tetramethylbenzidine (TMB) was used as an active radical oxygen species (ROS) indicator for the nanoceria catalyst before and after the cyanosilylation reaction of acetophenone **1** with TMSCN **2** [16e]. Absorption UV–visible spectroscopic measurements of the solutions (Fig. S8) show the expected band for protonated TMB at ~ 450 nm (a yellow colour solution is also visible by the naked eye) and the absence of any band indicative of TMB oxidation with ROS, at 650 nm (blue colour by the naked eye). This simple test confirms the lack of ROS in nanoceria during the catalyzed reaction.

Once determined that the catalytic activity of nanoceria does not come from particular crystalline faces nor oxygen vacancies, the role of Lewis and Brönsted acid sites in nanoceria during the cyanosilylation reaction was studied. Fig. 4 shows the catalytic results with nanoceria after addition of 10 mol% of either pyridine or di-*tert*-butylpyridine. While the former quenches the Lewis and Brönsted sites, the latter only quenches the Brönsted sites, and the results show that both amine bases decrease significantly the catalytic activity of nanoceria, particularly pyridine.

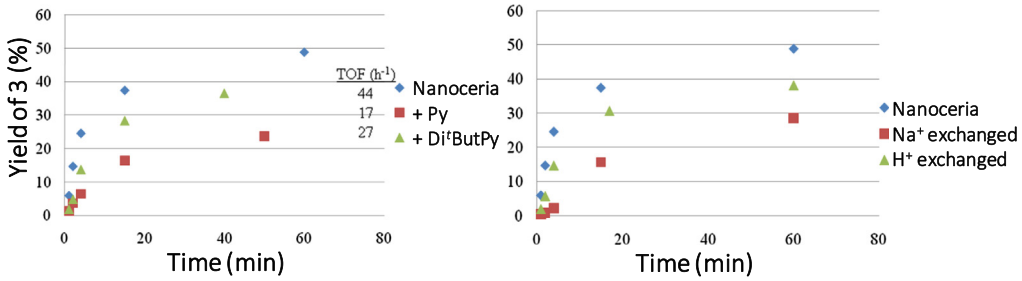

Fig. 4. (A) Kinetics for the cyanosilylation reaction of acetophenone **1** with TMSCN **2** after adding different pyridine quenchers (10 mol%), and (B) nanoceria exchanged with Na^+ and exchanged back with H^+.

Fig. 4 also shows that if the H^+ in nanoceria is exchanged by Na^+ [19], the catalytic activity decreases considerably, and this catalytic activity is partially recovered after exchanging back the H^+ cations. Calcination of nanoceria under a H_2 atmosphere prior to reaction (Fig. S3, right) dramatically decreases the catalytic activity, which also supports the presence of catalytically active and reducible Lewis metal sites in nanoceria. These results, together, strongly suggest that the catalytic activity of nanoceria for the cyanosilylation reaction comes from both Lewis and Brönsted acid sites [20].

The sharp stopping of the catalytic activity of nanoceria during the cyanosilylation reaction, at ~60% conversion, could in part be explained by the deposition of silicon and aminated organic molecules on the acid sites, thus blocking further catalytic cycles [20c]. However, a somewhat unexpected morphological issue was found during the examination of nanoceria after reaction. Fig. 5 shows a HR-TEM image with the corresponding energy-dispersive X-ray spectroscopy (EDS) mapping of a catalytic nanoceria rod after reaction, where an external layer containing a cerium/oxygen ratio slightly higher than in the bulk can be clearly seen, indicative of the presence of oxygen vacancies on surface. These catalytically inactive nanoceria phase, plenty of oxygen vacancies, can be generated by the release of HCN during reaction, just as HCl does, and explains the rapid deactivation of the nanoceria catalyst [13a,21]. Indeed, the recovery of the catalytic activity after calcination under air at 400 °C (see above) supports this explanation, since this air calcination regenerates the oxygen sites and restore the original catalytic material [22].

Fig. 6 shows the scope of the cyanosilylation reaction with TMSCN **2** for different ketones **4–16**, using commercially available nanoceria as a catalyst. The results show that TMS-protected cyanohydrins with aryl (products **17–18**), alkyl (products **22–27**) and alkenyl (products **28–29**) substituents can be formed in good

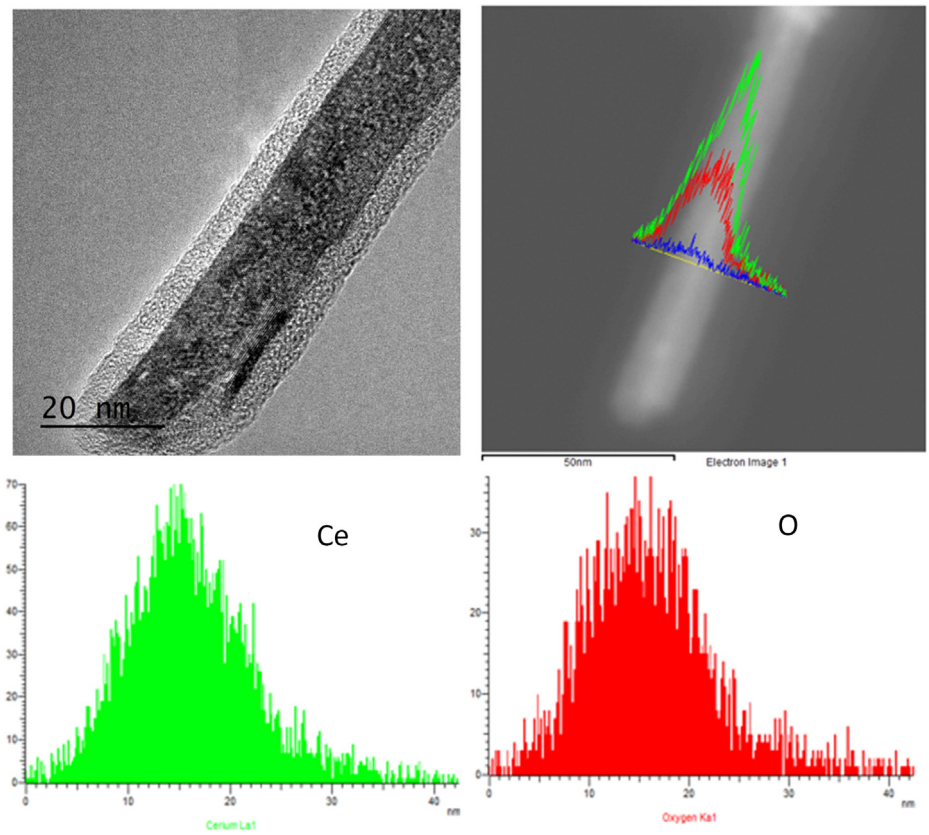

Fig. 5. HR-TEM with energy dispersive X-ray spectroscopy (EDS) of a representative ceria nanorod after reaction. The formation of an amorphous layer around the nanorod, just where the catalytic events have occurred, is clearly observed. EDS analysis shows a slight increase in the Ce/O ratio of the amorphous area, notice the lower green-to-red intensity ratio in the amorphous shell, so the generation of catalytically inactive oxygen vacancies can be inferred.

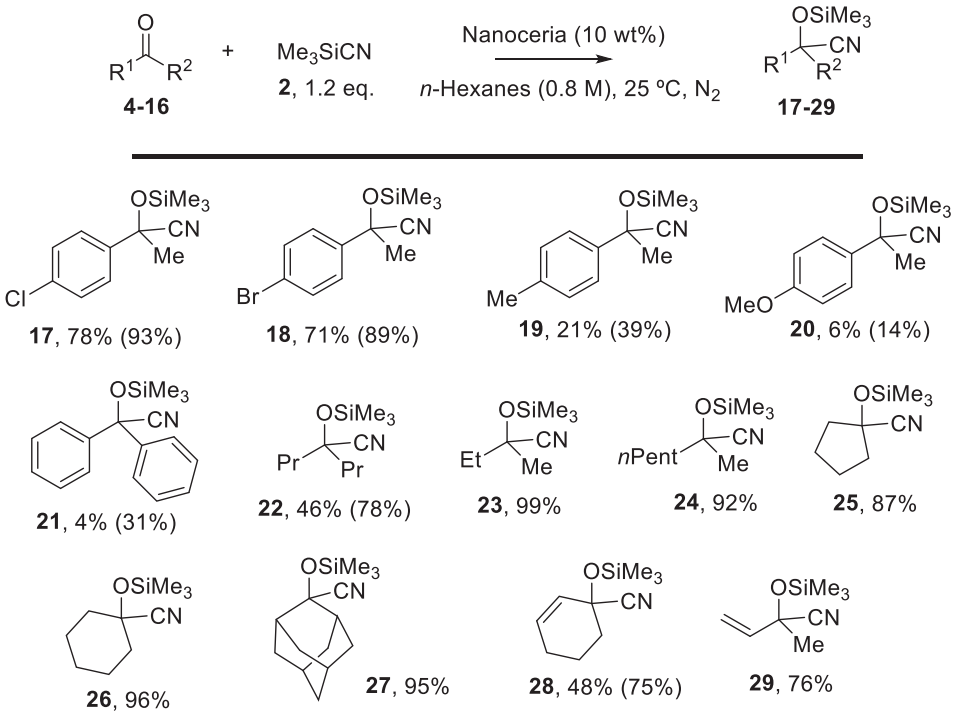

Fig. 6. Scope of the cyanosilylation reaction of ketones **4–16** with TMSCN **2** catalyzed by nanoceria at 25 °C for 1 h under inert atmosphere (yields after 24 h reaction time in parentheses).

to excellent yields. However, electron-donor substituents (products **19–21**) tend to hamper the reaction. Indeed, when an equimolecular amount of anisole is added to the highly reactive ketone adamantone **14**, the formation of the corresponding product **27** is nearly stopped (Fig. S9). A Hammett plot with different substituents in the *para*-position of acetophenone **1** shows a $\rho > 0$, which corresponds to a nucleophilic reaction, and a clear correlation with the σ^+ parameters indicates building of positive charge in the transition state, most probably the activation of the carbonyl group of the ketone (Fig. S10). The approximation of $\rho = 0$ for

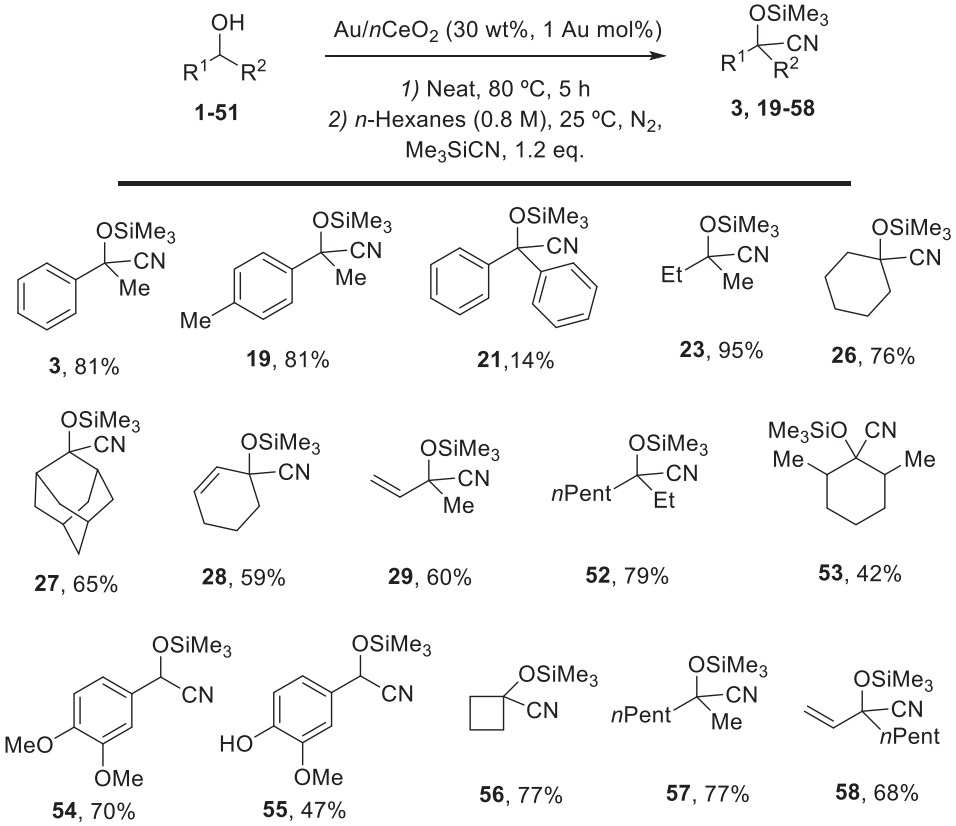

Fig. 7. Scope for the aerobic oxidation of alcohols/cyanosilylation reaction catalyzed by Au/nCeO$_2$ at 25 °C for 5 h under inert atmosphere. Two-step combined GC yields.

halide substituents is indicative that the activation of TMSCN **2** takes control at some point on the cyanosilylation rate, in accordance with the expected acid/base mechanism of the reaction.

3.2. Aerobic oxidation of alcohols/cyanosilylation reaction catalyzed by Au-$nCeO_2$

A sustainable organic synthesis demands the optimization of chemical steps during reaction, if possible by grouping several steps in one-pot and, ideally, over a recoverable solid catalyst [23]. In view that the cyanosilylation reaction proceeds in both catalytic amorphous and crystalline nanoceria, even under air, it was envisioned here the use of metal-supported nanoceria catalysts as bifunctional catalysts for the aerobic oxidation/cyanosilylation reactions [24]. In this way, nanoceria will act as both catalyst and support, enabling the cyanosilylation reaction after the metal-catalyzed oxidation reaction. This approach does not only engage two very different catalytic reactions, i.e. a dehydrogenation reaction mediated by ROS and a typical Lewis acid-catalyzed reaction [25], but also the activation of the bifunctional solid, since one single calcination of the solid will concomitantly fix the metal phase on the nanoceria surface, after impregnation with the metal precursor, and also activate the nanoceria framework for the cyanosilylation reaction, thus saving catalyst preparation steps.

Gold NPs on nanoceria (Au/$n$$CeO_2$, 5 Au wt%), prepared by a reported procedure with the commercial nanoceria catalyst active for the cyanosilylation reaction as a support [24a], was chosen as a model catalyst for the one-pot reaction. First, Au/$n$$CeO_2$ was tested in the aerobic oxidation of different alcohols, and the results show that the corresponding aldehydes and ketones are obtained in excellent yields with 1 Au mol% (Fig. S11). Then, Au/$n$$CeO_2$ was tested as a catalyst for the cyanosilylation reaction of acetophenone **1**, with the amount of catalyst required for complete alcohol oxidation (1 Au mol%, 30 $n$$CeO_2$ wt%) and under optimized conditions (see above), to give 81% yield of cyanohydrin **3**, a better yield than the corresponding bare nanoceria catalyst under the same reaction conditions (56%). With this encouraging result in hand, the Au/$n$$CeO_2$ catalyst was employed for both aerobic oxidation/-cyanosilylation reactions. The results for different alcohols are shown in Fig. 7. Good to excellent yields were obtained in most cases, which demonstrates that two mechanistically different metal NP- and nanoceria-catalyzed reactions are compatible over a same metal-supported nanoceria catalyst.

4. Conclusions

Nanoceria catalyzes the cyanosilylation of different ketones at temperatures between 0 and 50 °C and in high yields, even under solventless conditions. After simple calcination, the solid catalyst can be reused ten times without depletion of the catalytic activity. Other inorganic nano-oxides tested did not show this catalytic behavior. Different types of crystalline nanoceria, including amorphous nanoceria, are catalytically active, and these results enable the use of Au-supported nanoceria as a catalyst for aerobic oxidation of alcohols/cyanosilylation reactions. These results open the gate for the concomitant use of nanoceria-based materials as oxidation and Lewis catalysts, to design cascade reactions of utility in sustainable organic synthesis.

Declaration of Competing Interest

The authors declare that they have no known competing financial interests or personal relationships that could have appeared to influence the work reported in this paper.

Acknowledgements

Financial support by MINECO (Spain) (Project CTQ 2017-86735-P and Excellence Unit “Severo Ochoa” SEV-2016-0683) is acknowledged. F.G.-P. thanks ITQ for a contract and M.A.R-C. thanks Iberdrola Foundation for a fellowship.

Appendix A. Supplementary material

Supplementary data to this article can be found online at https://doi.org/10.1016/j.jcat.2020.09.032.

References

[1] For recent examples see: a) X.-P. Zeng, Z.-Y. Cao, X. Wang, L. Chen, F. Zhou, F. Zhu, C.-H. Wang, J. Zhou J. Am. Chem. Soc., 138 (1) (2016), pp. 416–425, 10.1021/jacs.5b11476. b) W. Wang, M. Lou, J. Li, S. A. Pullarkat, M. Ma Chem. Commun., 54 (24) (2018), pp. 3042–3044, 10.1039/c8cc00826d. c) L. Bao, X. Kong, Y. Wang Asian J. Org. Chem., 9 (5) (2020), pp. 757–760, 10.1002/ajoc.202000216. d) W.-Z. Wu, X.-P. Zeng, J. Zhou J. Org. Chem., (2020), Ahead of Print, 10.1021/acs.joc.9b03347.

[2] R.J.H. Gregory, Chem. Rev. 99 (1999) 3649, https://doi.org/10.1021/cr9902906.

[3] a) T.L. Adelsbach, R.S. Tjeerdema, Rev. Environ. Contam. Toxicol., 176 (2002), pp. 137, 10.1007/978-1-4899-7283-5_3. b) A.B. Smith, T. Tomioka, C.A. Risatti, J.B. Sperry, C. Sfouggatakis Org. Lett., 10 (2008), pp. 4359, 10.1021/ol801792k.

[4] a) D.A. Evans, L.K. Truesdale, G.L. Carroll J.C.S. Chem. Comm., (1973), pp. 55–56, 10.1039/c39730000055. b) K. Manju, S. Trehan J. Chem. Soc., Perkin Trans. 1, (1995), pp. 2383–2384, 10.1039/P19950002383. c) G.K.S. Prakash, H. Vaghoo, C. Panja, V. Surampudi, R. Kultyshev, T. Mathew, G.A. Olah PNAS, 104 (2007), pp. 3026–3030, 10.1073/pnas.0611309104.

[5] a) Y. Kikukawa, K. Suzuki, M. Sugawa, T. Hirano, K. Kamata, K. Yamaguchi, N. Mizuno Angew. Chem., Int. Ed., 51 (2012), pp. 3686–3690, 10.1002/ange.201200486. b) S. Rojas–Buzo, P. Garcia–Garcia, A. Corma ChemCatChem., 9 (6) (2017), pp. 997–1004, 10.1002/cctc.201601407. c) S. Zhang, B. Zhang, H. Liang, Y. Liu, Y. Qiao, Y. Qin Angew. Chem. Int. Ed., 57 (4) (2018), pp. 1091–1095, 10.1002/anie.201712010 d) Y.M. Nie, S. H. Li, M. Y. Lin, Jun. Chem. Commun., 56 (26) (2020), pp. 3809–3812, 10.1039/d0cc01216e.

[6] R. Dasgupta, S. Das, S. Hiwase, S.K. Pati, S. Khan, Organometallics, 38 (7) (2019), pp. 1429–1435, 10.1021/acs.organomet.8b00673. b) J. Yin, H. Fei Dalton Trans., 47 (12) (2018), pp. 4054–4058, 10.1039/c8dt00188j. c) B. Thirupathi, M.K. Patil, B.M.B.M. Reddy Applied Catalysis, A: General, 384 (1–2) (2010), pp. 147–153, 10.1016/j.apcata.2010.06.019.

[7] M.Á. Rivero-Crespo, M. Tejeda-Serrano, H. Pérez-Sánchez, J.P. Cerón-Carrasco, A. Leyva-Pérez, Angew. Chem. Int. Ed. 59 (2020) 3846–3849, https://doi.org/10.1002/anie.201909597.

[8] J. Oliver-Meseguer, A. Doménech-Carbó, M. Boronat, A. Leyva-Pérez, A. Corma, Angew. Chem. Int. Ed. 56 (2017) 6435–6439, https://doi.org/10.1002/anie.201700282.

[9] a) K. Higuchi, M. Onaka, Y. Izumi, J. Chem. Soc., Chem. Commun., 15 (1991), pp. 1035–1036, 10.1039/C39910001035. b) X. Huang, L. Chen, F. Ren, C. Yang, J. Li, K. Shi, X. Gou, W. Wang Synlett, 28 (4) (2017), pp. 439–444, 10.1055/s-0036-1588640.

[10] For recent reviews see: a) L. Liu, A. Corma, Chem. Rev. 118 (10) 2018, pp. 4981–5079, doi/10.1021/acs.chemrev.7b00776. b) J. M. Asensio, D. Bouzouita, P. W. N. M. van Leeuwen, B. Chaudret Chem. Rev., 120 (2) (2020), pp. 1042–1084, 10.1021/acs.chemrev.9b00368. c) M. Viciano–Chumillas, M. Mon, J. Ferrando–Soria, A. Corma, A. Leyva–Perez, D. Armentano, E. Pardo Acc. Chem. Res., 53 (2020), pp. 520–531, 10.1021/acs.accounts.9b00609.

[11] a) M. Tejeda–Serrano, M. Mon, B. Ross, F. Gonell, J. Ferrando–Soria, A. Corma, A. Leyva–Pérez, D. Armentano, E. Pardo J. Am. Chem. Soc., 140 (2018), pp. 8827−8832, 10.1021/jacs.8b04669. b) M.A. Rivero–Crespo, J. Oliver–Meseguer, K. Kaposka, P. Kutrowski, E. Pardo, J.P. Cerón–Carrasco, A. Leyva–Perez, Chem. Sci., 11 (2020), pp. 8113–8124, 10.1039/D0SC02391D. c) T. Ribeiro, A.S. Rodrigues, S. Calderon, A. Fidalgo, J.L.M. Gonçalves, V. André, M.T. Duarte, P.J. Ferreira, J.P.S. Farinha, C. Baleizão J. Colloid Interface Sc., 561 (2020), pp. 609–619, 10.1016/j.jcis.2019.11.036.

[12] For recent reviews on catalytic ceria see: a) W. Yang, X. Wang, S. Song, H. Zhang Chem, 5 (7) (2019), pp. 1743–1774, 10.1016/j.chempr.2019.04.009. b) K. Chang, H. Zhang, M. Cheng, Q. Lu ACS Catal., 10 (1) (2020), pp. 613–63, 10.1021/acscatal.9b03935. c) R. Schmitt, A. Nenning, O. Kraynis, R. Korobko, A. I. Frenkel, I. Lubomirsky, S.M. Haile, J.L.M. Rupp Chem. Soc. Rev., 49 (2) (2020), pp. 554–592, 10.1039/c9cs00588a. For an article on commercially available nanoceria characterization see d) M. Tinoco, S. Fernandez–Garcia, A. Villa, J.M. Gonzalez, G. Blanco, A.B. Hungria, L. Jiang, L. Prati, J.J. Calvino, X. Chen Catal. Sci. Technol., 9 (2019), pp. 2328–2334, 10.1039/C9CY00273A.

[13] F. Bozon-Verduraz, A. Bensalem, J. Chem. Soc., Faraday Trans. 90 (1994) 653–657, https://doi.org/10.1039/FT9949000653.

[14] a) A. Leyva-Pérez, D. Cómbita-Merchán, J.R. Cabrero-Antonino, S.I. Al-Resayes, A. Corma, ACS Catal., 3 (2013), pp. 250−258, 10.1021/cs300644s. b) A. Trovarelli, J. Llorca, ACS Catalysis, 7 (7) (2017), pp. 4716–4735, 10.1021/acscatal.7b01246.

[15] H.-X. Mai, L.D. Sun, Y.W. Zhang, R. Si, W. Feng, H.P. Zhang, H.C. Liu, C.H. Yan, J. Phys. Chem. B 109 (2005) 24380–24385, https://doi.org/10.1021/jp055584b.

[16] a) M. Nolan, S.C. Parker, G. W. Watson Surface Science, 595 (2005), pp. 223–232, 10.1016/j.susc.2005.08.015. b) T. López-Ausens, M. Boronat, P. Concepción, S. Chouzier, S. Mastroianni, A. Corma. J. Catal. 344 (2016), pp. 334–345. 0.1016/j.jcat.2016.09.032. c) K. Werner, X. Weng, F. Calaza, M. Sterrer, T. Kropp, J. Paier, J. Sauer, M. Wilde, K. Fukutani, S. Shaikhutdinov, H.–J. Freund J. Am. Chem. Soc., 139 (2017), pp. 17608−17616, 10.1021/jacs.7b10021. d) Z. Vajglova, R. Hemery, N. Kumar, K. Eränen, M. Peurla, J. Peltonen, J. Wärnå, J. Pérez–Ramírez, T. Salmi, D. Yu. Murzin J. Catal., 372 (2019), pp. 287–298, 10.1016/j.jcat.2019.03.009. e) J. Yang, S. Peng, Y. Shi, S. Ma, H. Ding, G. Rupprechter, J. Wang. J. Catal., 389 (2020), pp. 71–77, 10.1016/j.jcat.2020.05.016.

[17] a) M. Aresta, A. Dibenedetto, C. Pastore, C. Cuocci, B. Aresta, S. Cometa, E. De Giglio Catal. Today, 137 (2008), pp. 125–131, 10.1016/j.cattod.2008.04.043. For a recent review of bifunctional catalysts see. b) P. W. N. M. van Leeuwen, I. Cano, Z. Freixa ChemCatChem, 12 (2020), 10.1002/cctc.202000493.

[18] J. Soria, J.C. Conesa, A. Martinez-Arias, Colloids Surf. 158 (1999) 67–74, https://doi.org/10.1016/S0927-7757(99)00132-6.

[19] K. Nakajima, Y. Baba, R. Noma, M. Kitano, J.N. Kondo, S. Hayashi, M. Hara, J. Am. Chem. Soc. 133 (2011) 4224–4227, https://doi.org/10.1021/ja110482r.

[20] a) Y. Wang, F. Wang, Q. Song, Q. Xin, S. Xu, J. Xu J. Am. Chem. Soc., 135 (2013), pp. 1506–1515, 10.1021/ja310498c. b) G. Wang, L. Wang, X. Fei, Y. Zhou, R. F. Sabirianov, W. N. Mei, C. L. Cheung, Catal. Sci. Technol., 3 (2013), pp. 2602–2609, 10.1039/C3CY00196B.

[21] a) M. Scharfe, M. Capdevila-Cortada, V.A. Kondratenko, E.V. Kondratenko, S. Colussi, A. Trovarelli, N. López, J. Pérez-Ramírez ACS Catal., 8 (2018), pp. 2651–2663, 10.1021/acscatal.7b04431. b) V. Paunović, G. Zichittella, S. Mitchell, R. Hauert, J. Pérez-Ramírez, ACS Catal., 8 (2018), pp. 291–303, 10.1021/acscatal.7b03074.

[22] L. Vivier, D. Duprez, ChemSusChem 3 (2010) 654–678, https://doi.org/10.1002/cssc.201000054.

[23] A. Leyva-Pérez, P. García-García, A. Corma, Angew. Chem. Int. Ed. 53 (2014) 8687–8690, https://doi.org/10.1002/anie.201403049.

[24] a) A. Abad, P. Concepción, A. Corma, H. García Angew. Chem. Int. Ed., 44 (2005), pp. 4066–4069, 10.1002/anie.200500382. b) A. Leyva-Perez, J. Oliver-Meseguer, J.R. Cabrero-Antonino, P. Rubio-Marques, P. Serna, S. Al-Resayes, A. Corma ACS Catal., 3 (8) (2013), pp. 1865–1873, 10.1021/cs400362c. c) P. Rubio-Marques, J.C. Hernandez-Garrido, A. Leyva-Perez, A. Corma Chem. Commun. 50 (14) (2014), pp. 1645–1647, 10.1039/C3CC47693F. d) J. Oliver-Meseguer, I. Dominguez, R. Gavara, A. Leyva-Perez, A. Corma ChemCatChem, 9 (8) (2017), pp. 1429–1435, 10.1002/cctc.201700037. e) J. Oliver-Meseguer, I. Dominguez, R. Gavara, A. Domenech-Carbo, J.M. Gonzalez-Calbet, A. Leyva-Perez, A. Corma Chem. Commun., 53 (6) (2017), pp. 1116–1119, 10.1039/c3cc44104k. f) Q. Gu, W.-H. Fang, R. Wischert, W-J. Zhou, C. Michel, M. Pera-Titus. J. Catal. 380 (2019), pp. 132–144. 10.1016/j.jcat.2019.10.017.

[25] a) S. Zhang, Z.-Q. Huang, Y. Ma, W. Gao, J. Li, F. Cao, L. Li, C.-R. Chang, Y. Qu. Nat. Commun., 8 (2017), pp. 15266, 10.1038/ncomms15266. b) H. Wang, S. Luo, M. Zhang, W. Liu, X. Wub, S. Liu. J. Catal. 368 (2018), pp. 365–378. 10.1016/j.jcat.2018.10.018. c) M. Tamura, K. Tomishige. J. Catal. 389 (2020), pp. 285–296. 10.1016/j.jcat.2020.05.031.